

Domain Adaptation with Randomized Expectation Maximization

Twan van Laarhoven tvanlaarhoven@cs.ru.nl
Elena Marchiori elenam@cs.ru.nl
Radboud University, Postbus 9010, 6500GL Nijmegen, The Netherlands

March 22, 2018

Abstract

Domain adaptation (DA) is the task of classifying an unlabeled dataset (target) using a labeled dataset (source) from a related domain. The majority of successful DA methods try to directly match the distributions of the source and target data by transforming the feature space. Despite their success, state of the art methods based on this approach are either involved or unable to directly scale to data with many features. This article shows that domain adaptation can be successfully performed by using a very simple randomized expectation maximization (EM) method. We consider two instances of the method, which involve logistic regression and support vector machine, respectively. The underlying assumption of the proposed method is the existence of a good single linear classifier for both source and target domain. The potential limitations of this assumption are alleviated by the flexibility of the method, which can directly incorporate deep features extracted from a pre-trained deep neural network. The resulting algorithm is strikingly easy to implement and apply. We test its performance on 36 real-life adaptation tasks over text and image data with diverse characteristics. The method achieves state-of-the-art results, competitive with those of involved end-to-end deep transfer-learning methods.

Source code is available at <http://github.com/twanvl/adrem>.

1 Introduction

Domain adaptation (DA) addresses the problem of building a good predictor for a target domain using labeled training data from a related source domain and target unlabeled training data. A typical example in visual object recognition involves two different datasets consisting of images taken under different cameras or conditions: for instance, one dataset consists of images taken at home with a digital camera while another dataset contains images taken in a controlled environment with studio lightning conditions.

A natural formulation of the DA problem is: finding a model performing well on both source and target data. Without any prior knowledge (that is, with a uniform prior on each model), the source classifier is the best expected choice. In order to do ‘better’ on the target domain, one needs to incorporate some other desirable property.

A desirable property adopted by most DA methods is the ‘small domain discrepancy’. The popularity of this property is grounded on theoretical results on domain adaptation, which

showed that the domain discrepancy between source and target contributes to the target error (Ben-David et al., 2007, 2010).

Most current state-of-the-art methods reduce the discrepancy between source and target distributions using feature transformations. Simple methods based on this approach include Fernando et al. (2013); Gong et al. (2013); Sun et al. (2016). These methods have superquadratic complexity in the number of features, which is why they are not directly applied to high dimensional data. To overcome this problem feature selection on the source data is used, which reduces the predictive information for the target domain. For instance this phenomenon can happen in natural language processing, where different genres often use very different vocabulary to describe similar concepts. As classical example of this situation, consider product reviews retrieved from Amazon.com and the task of classifying them as positive or negative (sentiment polarity analysis): reviews of electronic type of products and reviews of dvd products use different vocabularies. Hence adaptation between these two domains (electronic and dvd) is rather challenging Blitzer et al. (2007).

Recently, end-to-end DA methods based on deep neural networks (DNN's), like Ganin et al. (2016); Sener et al. (2016); Long et al. (2016b), have been shown to perform very well on visual adaptation tasks. Training a DNN may require a large train data (Sener et al., 2016) as well as the use of target labeled data to tune parameters (Long et al., 2016b). Furthermore DNN's for domain adaptation can be sensitive to (hyper-)parameters of the learning procedure (Ganin et al., 2016). To address these issues, state of the art end-to-end DA methods fine tune deep neural networks which were trained on related very large data. For instance, in DA for visual object recognition, deep neural networks pre-trained on the Imagenet dataset are used, such as VGG (Simonyan and Zisserman, 2014).

Pre-trained DNN's have been used also to enhance the performance of DA methods based on shallow neural network architectures, like linear support vector machines (SVM's) (e.g. Sun et al., 2016). In this setting, a pre-trained DNN is employed in a pre-processing step to generate a non-linear representation of the input space based on deep features. However, as we will also show in our experimental analysis, shallow methods based on domain discrepancy have a limited positive effect when applied to deep features.

Although impressive results on domain adaptation have been achieved in the past decade, drawbacks of the current state of the art motivate our investigation. Our goal is to develop a DA method that is very simple, scalable to many features, and competitive with end-to-end DNN methods when used with deep features.

To this aim we re-visit an old friend of the machine learning community: the Expectation Maximization (EM) approach for labeled and unlabeled data (see e.g. McLachlan, 1975). The idea of this approach is to view the labels on unlabeled samples as missing data. Seeger (2000) provide an excellent review of this approach.

EM has been used in the past for semi-supervised learning Amini and Gallinari (2003); Nigam et al. (2006); Grandvalet and Bengio (2006); Smola et al. (2005) and self-training Ghahramani and Jordan (1994); Li et al. (2008); Tan et al. (2009); Bruzzone and Marconcini (2010). The so-called "hard" EM approach use provisional target label, while the "soft" EM one incorporates label confidences when fitting the model on the next iteration Margolis (2011). In self-training, the labeled data is used to train an initial model, which is then used to guess the labels or label probabilities of the unlabeled data. On the next round, the unlabeled data with provisional

labels (or label probabilities) are incorporated to train a new model. This procedure is iterated for a fixed number of times, or until convergence. Methods based on this approach differ in the way target samples are added and used. Some methods add only the samples with high label confidence at each iteration, e.g. Bruzzone and Marconcini (2010), while others use all the target data on each round, e.g. Li et al. (2008).

These methods have been significantly outperformed by more recent DA methods. A core reason of their sub-optimal performance is that EM suffers from the problem that poor label or label probability estimates on one round can lead to fast convergence to bad pseudo labels close to those estimated in the first E-step (Seeger, 2000; Margolis, 2011).

We propose to overcome the problem of fast convergence to bad pseudo labels by performing the M-step only on a random sub-sample of the target data. The size of the sample is then increased at each iteration until the entire target data is considered.

The only desirable property we embed in the method is ‘class balance’ to avoid degenerate solutions where all data have the same class label. We use a controlled random sampling which generates classes of equal size.

The resulting method, called Ad-REM (*Adaptation with Randomized EM*), uses the source labeled data to train an initial model (we consider a linear SVM or a logistic regression model), which is then used to guess the labels of the unlabeled target data. On the next round, a class-balanced random sub-sample the unlabeled target data with provisional labels is used to train a new model. The procedure is iterated for a fixed number of times. To reduce the variance due to the randomized procedure, we ensemble pseudo-labelings results over multiple runs.

Ad-REM is strikingly simple to implement and apply. It does not involve learning a transformation of the feature space, as in current state of the art (shallow) DA methods. Thus it is directly applicable to adaptation tasks which involve many variables. We show that on 12 adaptation tasks in natural language processing with many features Blitzer et al. (2007), where shallow methods like CORAL Sun et al. (2016) cannot be directly applied, a neat improvement is achieved by Ad-REM.

Ad-REM is extremely simple in comparison with end-to-end deep learning domain adaptation methods, which need large training data or rely on pre-trained deep models for weight initialization, and sometimes employ a small set of labelled target data for tuning their hyperparameters (Bousmalis et al., 2016; Long et al., 2016b). Ad-REM can be directly used with deep features from pre-trained DNN’s. We perform an extensive experimental analysis with three publicly available pre-trained DNN architectures. We show that using deep features, Ad-REM consistently achieves impressive results on object recognition adaptation tasks.

In particular, using ResNet deep features, Ad-REM achieves 96.7% average accuracy over the 12 adaptation tasks of the Office-Caltech 10 dataset, and 87.0% average accuracy over the 6 adaptation tasks of the Office 31 dataset (Saenko et al., 2010). On these datasets, current state of the art shallow method SA (Fernando et al., 2013) and CORAL (Sun et al., 2016) do not improve over the baseline SVM model without adaptation, while end-to-end deep DA methods achieve inferior performance.

Overall, results of experiments on 36 real-life adaptation tasks in visual object recognition and natural language demonstrate the state-of-the-art performance of Ad-REM.

In summary our contributions are: (1) a new DA method based on randomized EM; (2) two strikingly easy DA algorithms based on this method. These algorithms are (3) scalable to data with many features; (4) flexible to the use of deep features from pre-trained deep neural networks; (5) competitive or better than involved end-to-end deep learning DA algorithms.

These contributions provide renewed support to EM, as an easy and effective approach to perform domain adaptation.

2 Related work

For an in-depth description of the EM approach and methods for learning with labeled and unlabeled data we refer the reader to Seeger (2000). Algorithms based on the EM-approach are also well described by Margolis (2011, section 3.1.4). In particular, a self-training semi-supervised SVM algorithm has been introduced by Li et al. (2008). This EM-based algorithm iteratively re-trains a SVM classifier using an unlabeled dataset. At each iteration the unlabeled dataset is used for training with pseudo-labels computed from the model at the previous iteration. In the DA context, the use of the entire unlabelled (target) dataset to update the model at each iteration is ineffective, since it favors fast convergence to the source classifier, as we will show in next section.

The literature on DA is vast, for which we refer to survey papers like Margolis (2011); Pan and Yang (2010); Patel et al. (2015). Here we limit our description to few methods based on popular approaches.

Domain discrepancy reduction. The majority of the algorithms for DA try to reduce the discrepancy between source and target distributions using a data transformation. Popular and simple methods in this class include Fernando et al. (2013); Gong et al. (2013); Sun et al. (2016). For instance, CORrelation ALignment (CORAL) finds a linear transformation that minimizes the distance between the covariance of source and target. CORAL (Sun et al., 2016) uses a specific mapping and is not scalable for high number of features because it needs to compute and invert a covariance matrix. Subspace Alignment (SA) computes a linear map that minimizes the Frobenius norm of the difference between the source and target domains, which are represented by subspaces described by eigenvectors (Fernando et al., 2013). Gong et al. (2012) proposed a Geodesic Flow Kernel (GFK) which models domain shift by integrating an infinite number of subspaces that characterize changes in geometric and statistical properties from the source to the target domain. These methods learn a feature transformation and cannot be directly applied to high dimensional input data, since they have quadratic complexity in the number of features.

Importance weighting. Importance-weighting methods assign a weight to each source instance in such a way as to make the reweighed version of the source distribution as similar to the target distribution as possible (Shimodaira, 2000). Despite their theoretic appeal, importance-weighting approaches generally do not to perform very well when there is little “overlap” between the source and target domain.

Feature level adaptation. Feature level domain-adaptation methods either extend the source data and the target data with additional features that are similar in both domains (Blitzer et al., 2006). The more recent Feature Level Domain Adaptation (FLDA) method by Kouw et al.

(2016) models the dependence between the two domains by means of a feature-level transfer model that is trained to describe the transfer from source to target domain. FLDA assigns a data-dependent weight to each feature representing how informative it is in the target domain. To do it uses information on differences in feature presence between the source and the target domain.

Self training. The approach underlying self-training methods has been explained in the introduction. One of the first algorithms for domain adaptation based on this approach was introduced by Bruzzone and Marconcini (2010), which extended the formulation of support vector machines to domain adaptation. The method progressively adjusts an SVM classifier trained on the source data toward the target domain by replacing source samples with target samples having high confidence prediction. This way to update the classifier - choosing the most confidently labeled target samples according to the previous iteration’s estimation - although robust, yields a minor change the current belief, that is, the resulting classifier remains close to the source one. This is the reason why this method has been significantly outperformed by more recent DA algorithms which try to minimize domain discrepancy. Other methods based on this approach include the method by Habrard et al. (2013) which optimizes both the source classification error and margin constraints over the unlabeled target instances, and includes a regularization term to favor the reduction of the divergence between source and target distributions, and the methods by Germain et al. (2016) which derive DA bounds for the weighted majority vote framework that are used to infer principled DA algorithms.

End-to-end deep neural networks. Recently end-to-end DA methods based on deep neural networks have been shown to achieve impressive performance (Ganin et al., 2016; Sener et al., 2016; Long et al., 2016b). For instance, DLID (Chopra et al., 2013) is an end-to-end deep adaptation method which learns multiple intermediate representations along an interpolating path between the source and target domains. Deep Transfer Network (DTN) Zhang et al. (2015) employs a deep neural network to model and match both the domains marginal and conditional distributions. Residual Transfer Networks (RTN) Long et al. (2016b) performs feature adaptation by matching the feature distributions of multiple layers across domains. Deep-CORAL (Sun and Saenko, 2016) aligns correlations of layer activations in deep neural networks. Recently, adversarial learning has become a popular approach for domain adaptation. For instance, Tzeng et al. (2015) proposed adding a binary domain classifier to discriminate domain labels and a domain confusion loss to enforce its prediction to become close to a uniform distribution over binary labels. ReverseGrad (Ganin and Lempitsky, 2015; Ganin et al., 2016) enforces the domains to be indistinguishable by reversing the gradients of the the loss of the domain classifier. Joint Adaptation Networks (JAN) (Long et al., 2016a) aligns the joint distributions of multiple domain-specific layers across domains by means of a joint maximum mean discrepancy measure which is optimized using an adversarial learning procedure. Disadvantages of end-to-end DA methods based on deep neural networks are the need of large train data (Sener et al., 2016), the use of target labels to tune parameters (Long et al., 2016b) and their sensitivity to (hyper-)parameters of the learning procedure (Ganin et al., 2016).

Compared to recent state-of-the-art-algorithms, our method does not perform feature transformation or feature learning for adaptation, which is more effective in the presence of many features. This is also advantageous when deep features from pre-trained models are used, since it may be ineffective to match source and target distribution in such deep-feature space.

The superiority of our method in this setting is demonstrated by the results of our experiments. In particular, on visual object recognition, state of the art shallow methods like CORAL (Sun et al., 2016) and SA (Fernando et al., 2013) achieve little or no gain when used with deep features extracted from pre-trained neural networks, while our method outperforms involved end-to-end DNN algorithms like JAN (Long et al., 2016a)

3 Domain Adaptation with Randomized Expectation Maximization

We follow Margolis (2011) to explain the DA setting we use. We have a labeled (source) dataset $S = \{(\mathbf{x}_i^S, y_i^S)\}_{i=1}^{|S|}$ and an unlabeled (target) dataset $T = \{\mathbf{x}_i^T\}_{i=1}^{|T|}$. We want to maximize the observations of labeled source data S and unlabeled target data T , with the target labels as hidden variables. The EM objective is:

$$\underset{\mathbf{w}}{\text{maximize}} \sum_{i \in S} \log(p(x_i^S, y_i^S | \mathbf{w})) + \sum_{i \in T} \log E_{y_i^T | \mathbf{w}} \{p(x_i^T | y_i^T, \mathbf{w})\}.$$

The EM algorithm applied to this problem leads to a version of self-labeling with “soft” labels, where on iteration k , the E- and M-step are as follows:

E: Given a model $p(x, y | \mathbf{w}_k)$, compute $p(y_i^T = c | x_i^T, \mathbf{w}_k)$ for all x_i^T and all class labels c .

M: $\mathbf{w}_{k+1} = \text{argmax} \sum_{i \in S} \log(p(x_i^S, y_i^S | \mathbf{w})) + \lambda \sum_{i \in T} \log E_{y_i^T | \mathbf{w}_k} \{p(x_i^T | y_i^T, \mathbf{w})\}$.

Typically, \mathbf{w} is initialized on S , e.g. by maximizing $\sum_{i \in S} \log(p(x_i^S, y_i^S | \mathbf{w}))$.

In our domain adaptation context, optimization is also with respect to the labels of the target data, and the objective of hard EM becomes:

$$\underset{\mathbf{w}, y_i^T}{\text{maximize}} \sum_{i \in S} \log(p(x_i^S, y_i^S | \mathbf{w})) + \sum_{i \in T} \log p(x_i^T, y_i^T | \mathbf{w}). \quad (1)$$

This corresponds to a version of self-training with hard labels on T :

E: Given a model $p(x, y | \mathbf{w}_k)$, compute $y_i^T = \text{argmax}_c p(y_i^T = c | x_i^T, \mathbf{w}_k)$ for all x_i^T .

M: $\mathbf{w}_{k+1} = \text{argmax} \sum_{i \in S} \log(p(x_i^S, y_i^S | \mathbf{w})) + \sum_{i \in T} \log p(x_i^T | y_i^T, \mathbf{w})$.

The hard EM objective differs from the soft EM one in the second term computed over target domain examples: hard EM tries to maximize $p(x, y | \mathbf{w})$, whereas soft EM tries to maximize only $p(x | \mathbf{w})$.

The exact implementation of the maximization step depends on the model, we use logistic regression and SVM.

Logistic Regression (LR): The regularized log-likelihood for the logistic regression model is:

$$L_{LR}(\mathbf{w}) = \sum_{i \in S} \ell(\mathbf{w} \cdot x_i^S, y_i^S) - \log[1 + \exp(\mathbf{w} \cdot x_i^S)] + \sum_{i \in T} \ell(\mathbf{w} \cdot x_i^T, y_i^T) - \log[1 + \exp(\mathbf{w} \cdot x_i^T)] - \lambda \|\mathbf{w}\|^2, \quad (2)$$

where $\ell(z, y) = zy$.

The M-step of the self-training procedure for the LR model maximizes the function 2.

Support Vector Machine: Although SVM is not a probabilistic model, Grandvalet et al. (2006) showed that the hinge loss can be interpreted as the neg-log-likelihood of a semi-parametric model of posterior probabilities, while Franc et al. (2011) showed how the SVM can be viewed as a maximum likelihood estimate of a class of semi-parametric models. Therefore it is also ‘legal’ to use the SVM loss in our EM setting for DA:

$$L_{SVM}(\mathbf{w}) = C \sum_{i \in S} \ell(\mathbf{w} \cdot x_i^S, y_i^S) + C \sum_{i \in T} \ell(\mathbf{w} \cdot x_i^T, y_i^T) + \|\mathbf{w}\|_2^2, \quad (3)$$

where $\ell(z, y) = \max(0, 1 - yz)$ is the hinge loss and $C > 0$ is a hyper-parameter.

The M-step of the self-training procedure for the SVM model maximizes the function 3.

The above described EM approach has been developed and used in semi-supervised learning, where labeled and unlabeled samples are drawn from the same distribution. This is not necessarily the case when doing domain adaptation, since the unlabeled target data comes from a related yet different domain than the labeled source data. A consequence is that EM style methods do too little exploration. The resulting classifier stays close to one trained on the source data, but this tends to be a poor local optimum when the target is different from the source.

We describe in the next sub-sections our proposal to overcome this problem: class-balanced random sub-sample selection. We use SVM to illustrate our approach. A similar reasoning applies for the LR model.

3.1 Class-balanced Randomized EM

To overcome the limitations of the EM to quickly converge to potentially bad local optima, we propose to add randomization. Our approach is based on two observations.

First of all, suppose that we have found an optimum $\hat{\mathbf{w}}$ of L for another sample \hat{T} from the target domain. Using the framework of empirical risk minimization it follows that $\hat{\mathbf{w}}$ also generalizes to new samples from the target domain. In particular, it will give a good classification of T .

Once we have a classification of the target samples, we can use it as y^T . Then (3) reduces to a standard supervised SVM loss, which is easy to optimize using off-the-self libraries.

This leaves the problem of finding an optimal classifier $\hat{\mathbf{w}}$ for a sample \hat{T} .

Our second observation is that the smaller the size of the target dataset, the closer the problem becomes to a standard support vector machine on the source data. In the extreme case, when $|T| = 0$, we can easily optimize L exactly. Conversely, if $|\hat{T}|$ is close to $|T|$ we expect that $\hat{\mathbf{w}}$ is a better classifier for T .

We therefore propose an iterative sampling strategy, where we gradually increase the size of the sample of target data on which (3) is optimized. Since we can not draw new samples from

the target domain, we instead draw samples from the given target dataset T .

Another problem with the EM-based optimization of L_{SVM} is that even the global optimum might not actually give a good classification of the target domain. In particular, if there is a large margin between the two domains, then separating all of the target domain into a single class often gives a low loss. This issue becomes especially apparent in high dimensions, where the amount of empty space between data points becomes larger.

A way to avoid this problem is to enforce class balance, that is, that each class occurs roughly equally often among the labels y^T . Here we enforce class balance through a sampling strategy: at each iteration of our EM method we use a controlled random selection of the sub-sample of the target data with current pseudo-labels to enforce class balance. This corresponds to the optimization of a modified SVM loss which includes class balance by assigning equal importance to all classes, rather than to all target domain samples. Denote by T_c the set of points that is assigned to class c in y^T , i.e. $T_c = \{i \mid y_i^T = c\}$. And denote by K the number of classes. Then we define the balanced DA SVM loss to be

$$L_{\text{balanced}}(\mathbf{w}) = C \sum_{i=1}^{|S|} \ell(\mathbf{w} \cdot \mathbf{x}_i^S, y_i^S) + \frac{C}{K} \sum_{c=1}^K \frac{|T|}{|T_c|} \sum_{i \in T_c} \ell(\mathbf{w} \cdot \mathbf{x}_i^T, y_i^T) + \|\mathbf{w}\|_2^2. \quad (4)$$

The resulting algorithm, which we call Ad-REM (Adaptation with Randomized EM), is shown in Algorithm 1.

The above balanced DA SVM loss is close to the transductive support vector machine (TSVM) one. The only difference is the way class-balanced is incorporated in the optimization problem: directly in the DA SVM loss and as a constraint in TSVM. No algorithm is known to efficiently find a globally optimal solution of the TSVM optimization problem (Joachims, 2006). Thus Ad-REM can be viewed as a randomized method to solve the TSVM optimization problem.

In Figure 1 we illustrate the execution of Ad-REM on a toy example. It can be clearly seen that as the algorithm progresses the loss decreases, and the number of correctly classified samples in the target domain increases. In this example the correct classifier clearly has a large margin, so it can be found by minimizing L_{SVM} .

In Figure 2 we illustrate the need of class balance. It can be seen that although without class balance the loss of SVM improves during the iterations, the target accuracy decreases.

Because Ad-REM uses random samples of the data, the results can depend on the exact samples chosen. To reduce the variance in the predictions we simply run the method multiple times, and take a majority vote of the resulting labelings. In all experiments we have used the ensemble-Ad-REM method, which is shown in Algorithm 2.

4 Experimental analysis

We perform extensive experiments on 36 adaptation tasks from real-life text and image benchmark datasets of diverse characteristics: with high number of features, relatively small sample

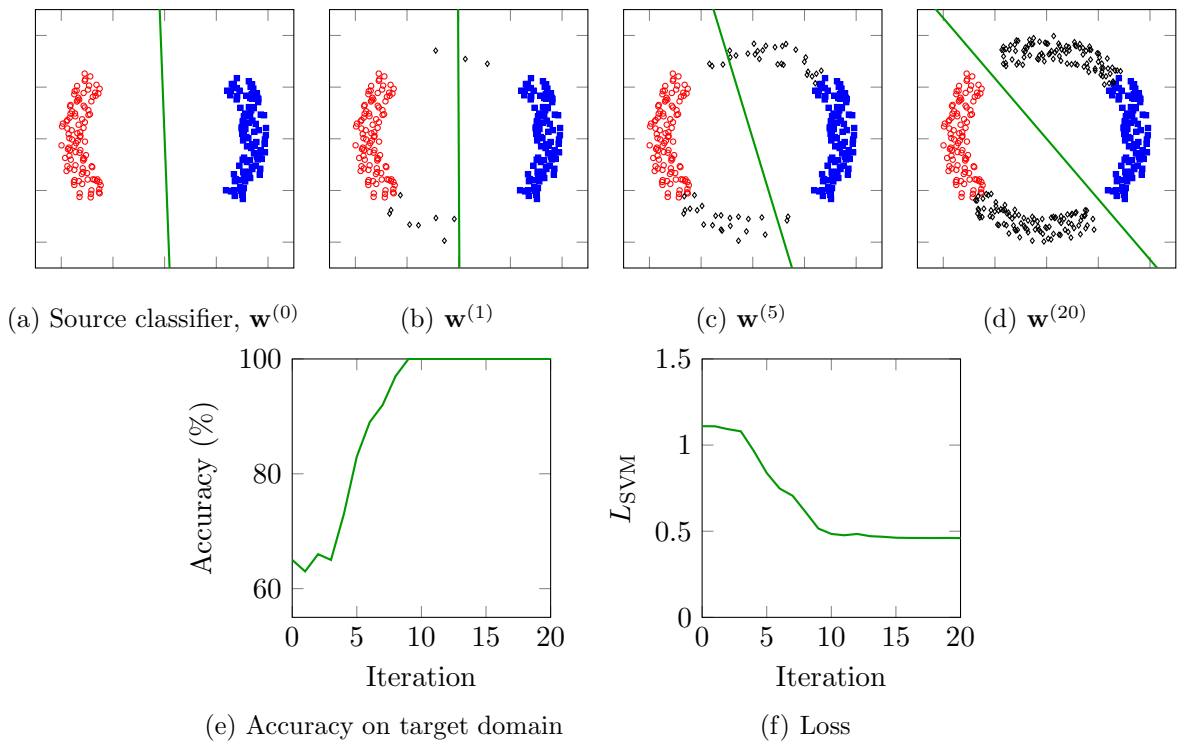


Figure 1: A toy example of domain adaptation. The source data span an arc of 80° for each class, and the target data is rotated 80° compared to the source, leaving a gap of 20° with the source data of the other class. (a)...(d) show the trained classifier over the iterations of Ad-REM, as larger samples are selected for training the SVM. (f) shows the SVM loss $L_{\text{SVM}}(\mathbf{w})$ over the iterations.

Algorithm 1 The single-Ad-REM method

Require: Source dataset $S = (\mathbf{x}^S, y^S)$; Target dataset $T = \mathbf{x}^T$; Regularization parameter C ; number of iterations M .
 $\mathbf{w}^{(0)} \leftarrow$ train SVM on S
 $y^{(0)} \leftarrow$ predict labels with $\mathbf{w}^{(0)}$ on T
for $k \leftarrow 1$ **to** M **do**
 $n_k \leftarrow \frac{k}{M}|T|$
 $B^{(k)} \leftarrow$ draw balanced subset of size n_k from $(\mathbf{x}^T, y^{(k-1)})$
 $\mathbf{w}^{(k)} \leftarrow$ train SVM on $\text{concat}(S, B^{(k)})$ % **M-step**
 $y^{(k)} \leftarrow$ predict labels with $\mathbf{w}^{(k)}$ on T % **E-step**
end for
return $y^{(M)}$

Algorithm 2 The ensemble-Ad-REM method

Require: Source dataset $S = (x^S, y^S)$; Target dataset $T = \mathbf{x}^T$; Regularization parameter C ; number of iterations M ; number of ensemble iterations m .
for $j \leftarrow 1$ **to** m **do**
 $z_j \leftarrow$ single-Ad-REM(S, T, C, M)
end for
return MajorityVote(z_1, z_2, \dots, z_m)

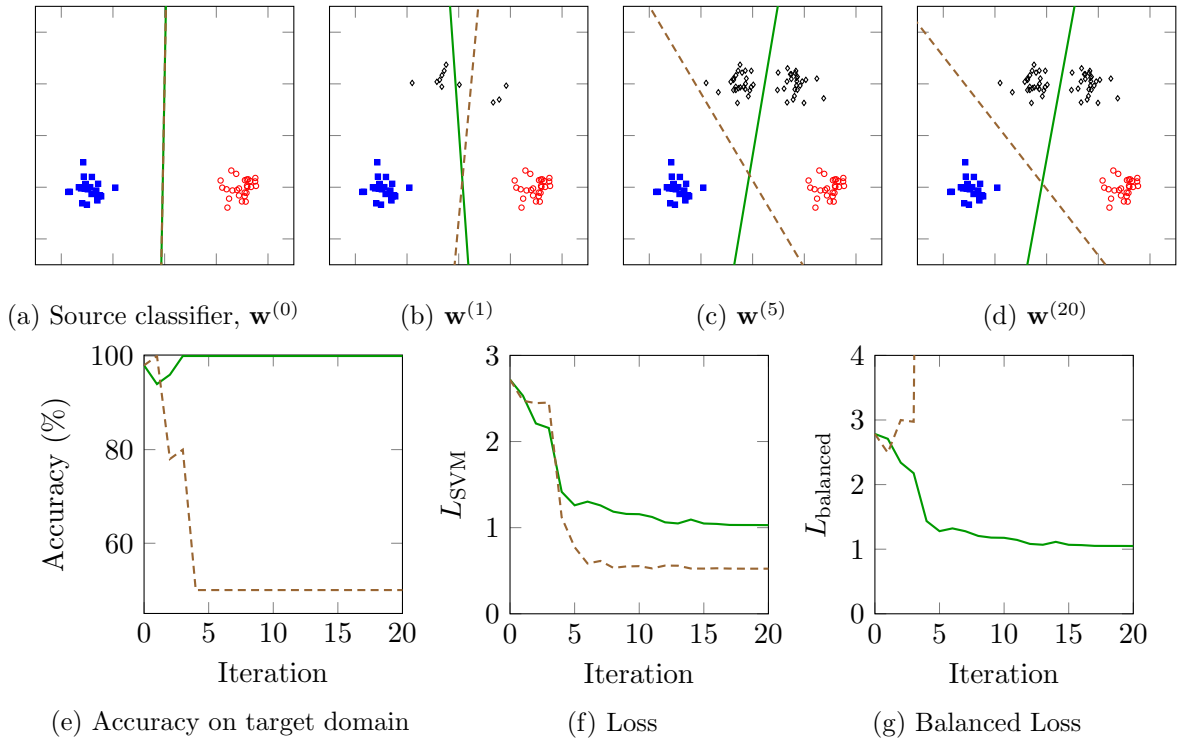


Figure 2: A toy example showing the need for balancing. The dashed brown classifier is trained without balancing, resulting in a better SVM loss, but a much lower accuracy.

size, larger number of classes and large scale data. Furthermore, on two visual domain adaptation datasets, we perform extensive experiments with deep features generated from existing pre-trained deep neural network classifiers.

In all experiments we assume target instances to be unlabeled. In Ad-REM we use an ensemble with 11 repetitions (we chose a prime number to prevent ties). For all runs we use 20 iterations. The parameter C is chosen with internal three-fold cross-validation on the source domain.

We use linear SVM and Logistic Regression (LR) as base classifiers, implemented by liblinear (Fan et al., 2008). Linear SVM and LR are our source hypothesis baselines that do not use domain adaptation. In our experiments with more than two classes, we used one-vs-all linear SVM and multi-class logistic regression.

We compare with popular state-of-the-art shallow DA methods, Subspace Alignment (SA) (Fernando et al., 2013), Feature Level Domain Adaptation (FLDA) (Kouw et al., 2016), and Correlation Alignment (CORAL) (Sun et al., 2016). The latter is the dominant state-of-the-art approach employing feature transformation.

Parameters for these shallow baselines are chosen with cross validation on the source dataset.

We assess all algorithms in a fully transductive setup where all unlabeled target instances are used during training for predicting their labels. We use labeled instances of the first domain as the source and unlabeled instances of the second domain as the target. We evaluate the accuracy on the target domain as the fraction of correctly labeled target instances.

We run experiments with source code of the shallow DA methods (except on the Office 31 dataset where we use results reported by Sun et al. (2016) which were obtained using the same evaluation protocol we use for Ad-REM).

We also assess the performance of Ad-REM and the shallow baselines on features extracted with a deep neural network. Specifically, we use the ResNet 50 architecture He et al. (2016) that was pre-trained on ImageNet. This network is available through Keras (Chollet et al., 2015). We rescale the images to 224×224 pixels, and pass these through the network. We then use the output of the nonlinearities on the last hidden layer as features.

4.1 Results

In the results reported in the sequel, we use $A \rightarrow B$ to indicate the adaptation task with A as source dataset and B as target one.

When results of a method are missing from a table it means either the method could not be run on such data (kept running for days) or the corresponding paper did not contain results of that method on the considered data.

Amazon sentiment dataset This dataset, introduced by Blitzer et al. (2007), has many features (over 47000), which are word unigram and bigram counts. It involves 4 domains, Books (B), Dvd (D), Electronics (E) and Kitchen (K), each with 1000 positive and 1000 negative examples obtained from the dichotomized 5-star rating. The considered shallow baselines have quadratic complexity in the number of features, which is why they can't be used in high-dimensional settings, such as the Amazon dataset. Therefore, these baselines have to

use feature selection: Gong et al. (2013) used feature selection to reduce the data set to 400 features. We conduct experiments with this dataset and validation protocol as in Sun et al. (2016): random subsamples of the source (1600 samples) and target (400 samples) data and standardized features. The experiment is repeated 20 times.

Feature selection might remove features relevant to the target. Keeping all features is possible in our method, which avoids this risk. Therefore we also report results of Ad-REM under the same experimental protocol but with *all* features. In this case we can not standardize the data, because that would destroy the sparsity, instead we normalize by dividing each feature by its standard deviation. To test the stability of the method we have repeated this experiment 10 times. Table 1 reports the mean and standard deviation of the accuracy, which shows that using all features improves accuracy.

Office-Caltech 10 object recognition dataset This dataset (Gong et al., 2012) consists of 10 classes of images from an office environment in 4 image domains: Webcam (W), DSLR (D), Amazon (A), and Caltech256 (C), with 958, 295, 157, 1123 instances, respectively. The dataset uses 800 SURF features, which we preprocess by dividing by the instance-wise mean followed by standardizing. We follow the standard protocol (Gong et al., 2012; Fernando et al., 2013; Sun et al., 2016), and use 20 labeled samples per class from the source domain (except for the DSLR source domain, for which we use 8 samples per class). We repeated these experiment 20 times, and report the mean and standard deviation of accuracy in Table 3.

On this dataset CORAL, FLDA and Ad-REM achieve comparable performance when SURF features are used. The improvement over the baseline is very small, and for some transfer tasks such as A→C, Ad-REM actually gives worse results than the baseline.

When using deep features, Ad-REM achieves best performance with a substantial increase in accuracy over no adaptation, while CORAL and FLDA do not improve over no adaptation. Using ResNet 50 deep features, Ad-REM achieves 12% gain in the accuracy on the C→W transfer task (from 86.0% to 98.1%). Overall, results indicate that the source classifier achieves excellent performance when applied to deep features. These results confirm that deep models trained on the very large ImageNet dataset generate powerful domain invariant features.

We have also performed experiments using the full source domain as training data, the results of this experiment are reported in Table 4. These results are very similar to the results with the standard protocol. With SURF features there is a noticeable increase in accuracy compared to the standard protocol, because more source data is available. For the deep features the differences are much smaller, because the accuracy was already high.

Office 31 dataset We next perform object recognition adaptation with a *larger number of classes* and deep features. We use the standard Office dataset 31 (Saenko et al., 2010) which contains 31 classes (the 10 from the Office-Caltech 10 plus 21 additional ones) in 3 domains: Webcam (W), DSLR (D), and Amazon (A). Office-31 has a total of 4110 instances, with a maximum of 2478 per domain over 31 classes. We run experiments using all labeled source and unlabeled target data.

On this dataset CORAL achieves best performance, slightly better than that of Ad-REM with LR as base classifier, only when using the DECAF-fc7 deep features by Tommasi and Tuytelaars (2014). When using deep features generated from the ResNet 50 architecture, Ad-REM outperforms all other methods, and obtains excellent performance, with a significant improvement

over no adaptation. The gain in the accuracy is rather large when performing adaptation over hard transfer tasks. For instance about 15% gain is achieved on $A \rightarrow W$ (from 73.8% to 89.4%) and about 12% on $D \rightarrow A$ (from 60.3% to 72.6%).

Cross Dataset Testbed Finally, we also consider a larger scale evaluation using the Cross Dataset Testbed (Tommasi and Tuytelaars, 2014), using deep features obtained with DECAF. The dataset contains 40 classes from 3 domains: 3847 images for the domain Caltech256 (C), 4000 images for Imagenet (I), and 2626 images for SUN (S). Results of these experiments are shown in Table 6. Also on this dataset Ad-REM obtains best results, and improves by a large margin over no adaptation. Previous papers have used standardization of the features.

We found it beneficial to increase sparsity by rectifying the inputs before normalization, that is, set negative values to 0 ($\max(0, x)$); and to then normalize by dividing by the standard deviation only. We see improved performance with rectified features compared to the original ones, likely because rectification was also used during the training of the neural network.

4.2 Comparison with end-to-end deep methods

For a direct comparison with state-of-the-art end-to-end DNN methods, we compare results of Ad-REM on the Office 31 dataset with published results of deep transfer methods based on ResNet: Deep Domain Confusion (DDC) (Tzeng et al., 2014), Deep Adaptation Network (DAN) (Long et al., 2015), Residual Transfer Networks (RTN) Long et al. (2016b), Reverse Gradient (RevGrad) Ganin and Lempitsky (2015); Ganin et al. (2016), and Joint Adaptation Networks (JAN) Long et al. (2016a). All comparing methods fine-tune the ResNet50 architecture pre-trained on ImageNet. RTN and JAN are not fully unsupervised and need a few labeled target data for hyperparameter optimization. These results are taken from Long et al. (2016a), and reported in Table 5.

4.3 Discussion

On almost linearly separable classification tasks, like sentiment polarity classification with text data, Ad-REM and the other shallow methods achieve comparable results when applied to a subset of pre-selected 400 features. However, Ad-REM can profit from the direct use of all 47000 features of this dataset, and achieve improved target accuracy, while the other shallow algorithms do not terminate or run out of memory when all features are used.

On harder classification tasks, like visual object detection, target accuracy performance does not differ substantially across shallow methods. In particular, when the performance of the source classifier on the target is low, like on the of the Office-Caltech 10 dataset with SURF features, performance of Ad-REM remains close to that of the source classifier, and is sometimes worse. This happens because a good starting point is needed for the algorithm to converge to a good local optimum.

Using deep features from pre-trained deep neural network models is highly beneficial for Ad-REM. In this case, the source classifier is good also for the target, and Ad-REM profits from this, especially on $A \rightarrow D$, $A \rightarrow W$ and $C \rightarrow W$, where it gains about 10% accuracy. On the other hand, the gain in accuracy obtained using other shallow DA methods is relatively small.

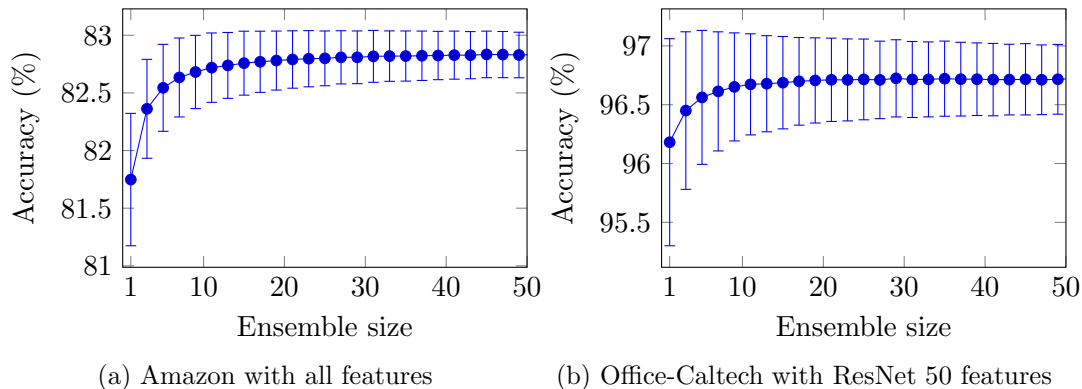


Figure 3: Accuracy as a function of ensemble size m . Average over all domain pairs, and 2000 repetitions. Error bars indicate standard deviation.

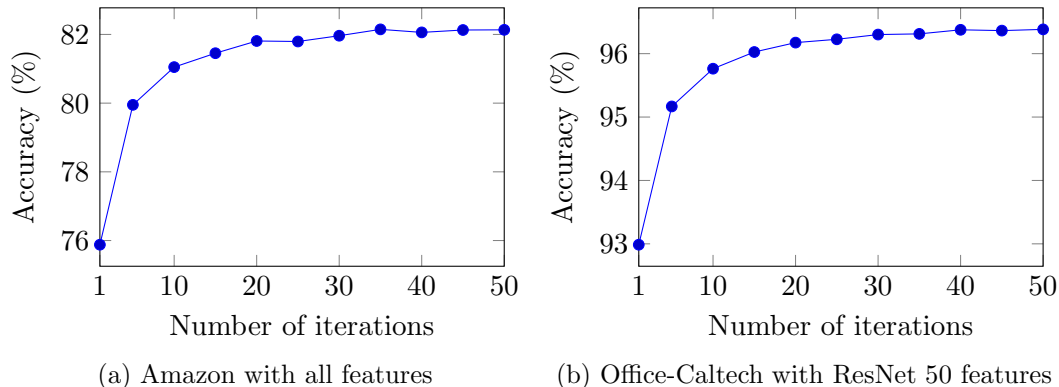


Figure 4: Accuracy as a function of number of iterations M . No ensemble is used.

Overall, results with deep features on the Office-Caltech 10 and Office 31 datasets show that the source classifier already achieves good performance when applied to deep features. These results confirm that deep models trained on the very large ImageNet dataset generate powerful domain invariant features.

4.4 Sensitivity analysis

In this paragraph we investigate the sensitivity of Ad-REM to its parameters.

First, in Figure 3 we plot the test set accuracy as a function of the ensemble size m . Ad-REM is a stochastic method, since it relies on bootstrap samples in each iterations. Using an ensemble is a way of reducing this variance. As expected, using a larger ensemble produces better results. The variance over multiple runs also becomes smaller with a larger ensemble size. For $m > 10$ there are diminishing returns to further increasing the ensemble size.

In Figure 4 we vary the number of iterations M , without using an ensemble ($m = 1$). Again, more iterations produce better results, since the algorithm has more time to converge to good labels on the target domain.

5 Conclusion

We introduced Ad-REM, a strikingly easy and effective method for DA. We showed that Ad-REM can be viewed as a EM-based method with a controlled random sampling strategy, which enforces class balance on the target domain during the optimization procedure.

Results of our experimental analysis lead to the following interesting conclusions: (1) EM can be successfully exploited in domain adaptation; (2) the direct combination of Ad-REM with deep learning features is highly beneficial and competitive with more involved end-to-end deep-transfer learning methods, notably on hard transfer tasks, such as $D \rightarrow A$ and $W \rightarrow A$ in the Office 31 dataset; (3) Ad-REM sets a new state-of-the-art on various transfer tasks with image as well as text data.

There are (at least) two limitations of our new approach for DA that remain to be investigated, which we summarize below.

Piecewise linearity. Ad-REM considers linear hypotheses generated by training SVM in the original feature space: the final majority vote model is a piecewise linear classifier. Therefore, for almost linearly separable tasks, like the adaptation tasks of the Amazon dataset, its performance is excellent. However, this may be a limitation in case of highly non-separable classification tasks. Results of our experiments showed that Ad-REM can directly profit from the used of deep features from pre-trained models in visual domain adaptation, with a significant increase in performance. It remains to be investigated whether it is even more beneficial to incorporate Ad-REM into an end-to-end deep learning architecture for DA or use a more powerful type of base classifier.

Fixed number of iterations. Our iterative EM-based procedure terminates after a number of iterations which are determined by the input parameter M . We showed in our sensitivity analysis that Ad-REM is robust with respect to the choice of M . However, there is no theoretical guarantee that the algorithm will have converged after M iterations. A natural extension of the method could be to let the algorithm proceed without sampling after the last iteration, as in the standard EM method. To still optimize the class balanced loss function, one could use weighting instead of biased sampling in these extra iterations. In practice the lack of convergence is not a problem, since there is already no guarantee of finding a global optimum. However, the effect of alternative and possibly more effective controlled random sampling strategies with guaranteed convergence remain to be investigated.

Acknowledgements

We would like to thank Baochen Sun for his prompt reply to our emails, in particular for providing interesting information about the application of CORAL.

This work has been partially funded by the Netherlands Organization for Scientific Research (NWO) within the EW TOP Compartment 1 project 612.001.352.

Table 1: Accuracy on the Amazon sentiment dataset using the standard protocol of Gong et al. (2013); Sun et al. (2016).

| | K→D | D→B | B→E | E→K | avg |
|--------------|-----------------|-----------------|-----------------|-----------------|-----------------|
| 400 features | | | | | |
| Source SVM | 73.3±1.9 | 78.3±2.3 | 75.6±1.5 | 83.1±1.8 | 77.6±1.1 |
| Source LR | 74.2±1.6 | 78.9±2.1 | 76.4±2.2 | 84.0±1.7 | 78.4±1.1 |
| SA | 73.3±1.9 | 78.3±2.3 | 75.6±1.5 | 83.1±1.8 | 77.6±1.1 |
| FLDA-L | 73.5±2.0 | 79.4±2.1 | 75.6±1.9 | 84.3±2.0 | 78.2±0.9 |
| FLDA-Q | 74.5±1.8 | 79.6±1.8 | 77.2±1.6 | 84.6±1.8 | 79.0±1.0 |
| CORAL | 73.5±1.8 | 78.3±2.0 | 76.1±1.7 | 83.1±1.9 | 77.7±0.8 |
| Ad-REM SVM | 73.7±1.5 | 78.4±2.0 | 76.9±2.1 | 83.5±1.8 | 78.1±0.8 |
| Ad-REM LR | 75.4±1.5 | 79.4±1.9 | 77.4±2.4 | 84.1±1.9 | 79.1±1.0 |
| All features | | | | | |
| Source SVM | 73.8±2.3 | 78.8±2.1 | 72.6±2.3 | 85.9±1.7 | 77.8±1.1 |
| Source LR | 74.3±2.4 | 79.9±2.1 | 72.9±2.3 | 86.4±1.9 | 78.4±1.1 |
| Ad-REM SVM | 76.3±2.6 | 81.0±2.3 | 79.0±2.7 | 86.1±2.0 | 80.6±1.3 |
| Ad-REM LR | 77.3±2.9 | 81.7±1.9 | 79.7±2.6 | 87.0±2.2 | 81.4±1.3 |

Table 2: Accuracy on the Amazon dataset using the full source and target domain. Mean and standard deviation over 10 runs.

| | B→D | B→E | B→K | D→B | D→E | D→K | E→B | E→D | E→K | K→B | K→D | K→E | avg |
|--------------|-------------|-------------|-------------|-------------|-------------|-------------|-------------|-------------|-------------|-------------|-------------|-------------|-------------|
| 400 features | | | | | | | | | | | | | |
| Source SVM | 77.5 | 76.4 | 78.2 | 78.2 | 75.3 | 78.2 | 73.8 | 73.1 | 83.2 | 74.3 | 73.6 | 82.7 | 77.0 |
| | ±0.0 | ±0.0 | ±0.0 | ±0.0 | ±0.0 | ±0.0 | ±0.0 | ±0.0 | ±0.0 | ±0.0 | ±0.0 | ±0.0 | ±0.0 |
| Source LR | 78.9 | 77.4 | 79.7 | 78.7 | 77.4 | 80.0 | 73.6 | 73.4 | 84.8 | 75.0 | 74.7 | 83.0 | 78.0 |
| | ±0.0 | ±0.0 | ±0.0 | ±0.0 | ±0.0 | ±0.0 | ±0.0 | ±0.0 | ±0.0 | ±0.0 | ±0.0 | ±0.0 | ±0.0 |
| SA | 77.5 | 76.4 | 78.2 | 78.2 | 75.3 | 78.2 | 73.8 | 73.1 | 83.2 | 74.3 | 73.6 | 82.7 | 77.0 |
| | ±0.0 | ±0.0 | ±0.0 | ±0.0 | ±0.0 | ±0.0 | ±0.0 | ±0.0 | ±0.0 | ±0.0 | ±0.0 | ±0.0 | ±0.0 |
| FLDA-L | 76.5 | 76.3 | 77.6 | 79.7 | 77.0 | 79.8 | 72.8 | 71.8 | 84.3 | 74.1 | 74.3 | 82.9 | 77.3 |
| | ±1.8 | ±1.7 | ±1.5 | ±0.5 | ±0.3 | ±0.3 | ±0.6 | ±2.2 | ±0.3 | ±0.7 | ±0.4 | ±0.4 | ±0.3 |
| FLDA-Q | 79.3 | 77.5 | 80.1 | 79.7 | 77.2 | 79.8 | 74.2 | 73.9 | 84.9 | 74.7 | 75.2 | 82.5 | 78.3 |
| | ±0.3 | ±0.4 | ±0.4 | ±0.4 | ±0.6 | ±0.3 | ±0.4 | ±0.4 | ±0.3 | ±0.3 | ±0.2 | ±0.3 | ±0.1 |
| CORAL | 78.1 | 76.7 | 78.4 | 78.8 | 76.4 | 78.3 | 74.8 | 73.9 | 83.6 | 74.8 | 74.4 | 82.9 | 77.6 |
| | ±0.0 | ±0.0 | ±0.0 | ±0.0 | ±0.0 | ±0.0 | ±0.0 | ±0.0 | ±0.0 | ±0.0 | ±0.0 | ±0.0 | ±0.0 |
| Ad-REM SVM | 78.0 | 79.2 | 81.9 | 78.5 | 79.4 | 80.9 | 74.6 | 75.2 | 84.1 | 76.7 | 75.4 | 81.5 | 78.8 |
| | ±0.2 | ±0.2 | ±0.2 | ±0.3 | ±0.2 | ±0.2 | ±0.1 | ±0.2 | ±0.1 | ±0.1 | ±0.4 | ±0.2 | ±0.1 |
| Ad-REM LR | 79.5 | 79.8 | 83.1 | 80.1 | 81.5 | 82.1 | 76.1 | 76.6 | 84.9 | 76.5 | 76.7 | 83.0 | 80.0 |
| | ±0.1 | ±0.1 | ±0.1 | ±0.1 | ±0.2 | ±0.1 | ±0.1 | ±0.1 | ±0.1 | ±0.2 | ±0.1 | ±0.1 | ±0.0 |
| All features | | | | | | | | | | | | | |
| Source SVM | 76.6 | 71.4 | 75.1 | 78.1 | 74.9 | 77.1 | 67.8 | 70.4 | 85.7 | 71.0 | 74.5 | 83.1 | 75.5 |
| | ±0.0 | ±0.0 | ±0.0 | ±0.0 | ±0.0 | ±0.0 | ±0.0 | ±0.0 | ±0.0 | ±0.0 | ±0.0 | ±0.0 | ±0.0 |
| Source LR | 77.7 | 70.5 | 75.6 | 78.9 | 74.3 | 76.9 | 69.0 | 70.5 | 85.9 | 72.1 | 74.4 | 83.0 | 75.7 |
| | ±0.0 | ±0.0 | ±0.0 | ±0.0 | ±0.0 | ±0.0 | ±0.0 | ±0.0 | ±0.0 | ±0.0 | ±0.0 | ±0.0 | ±0.0 |
| Ad-REM SVM | 81.8 | 84.5 | 86.0 | 83.2 | 85.1 | 86.3 | 76.1 | 78.6 | 87.5 | 78.1 | 80.4 | 85.3 | 82.7 |
| | ±0.3 | ±0.3 | ±0.4 | ±0.3 | ±0.4 | ±0.2 | ±0.4 | ±0.3 | ±0.3 | ±0.3 | ±0.3 | ±0.3 | ±0.1 |
| Ad-REM LR | 82.4 | 84.8 | 86.7 | 83.4 | 85.9 | 86.6 | 76.8 | 79.0 | 88.4 | 78.1 | 81.7 | 85.9 | 83.3 |
| | ±0.3 | ±0.4 | ±0.4 | ±0.3 | ±0.3 | ±0.3 | ±0.3 | ±0.3 | ±0.2 | ±0.4 | ±0.2 | ±0.2 | ±0.1 |

Table 3: Average accuracy on the Office-Caltech 10 dataset using the standard protocol of Gong et al. (2012); Fernando et al. (2013); Sun et al. (2016). We report standard deviations where available.

| | A→C | A→D | A→W | C→A | C→D | C→W | D→A | D→C | D→W | W→A | W→C | W→D | avg |
|---------------|---------------------|---------------------|---------------------|---------------------|---------------------|---------------------|---------------------|---------------------|---------------------|---------------------|---------------------|----------------------|---------------------|
| SURF features | | | | | | | | | | | | | |
| Source SVM | 36.3 ±1.6 | 36.7 ±3.3 | 35.9 ±2.5 | 45.0 ±2.2 | 42.1 ±3.3 | 39.1 ±3.8 | 34.6 ±1.0 | 32.1 ±0.9 | 75.8 ±2.4 | 37.9 ±0.5 | 33.9 ±1.2 | 73.5 ±3.4 | 43.6 ±1.0 |
| Source LR | 36.3 ±1.5 | 36.7 ±3.4 | 34.9 ±2.4 | 44.9 ±1.9 | 41.7 ±3.4 | 38.8 ±2.9 | 34.5 ±0.9 | 31.8 ±1.1 | 76.2 ±2.3 | 38.0 ±0.9 | 34.3 ±1.3 | 75.3 ±2.1 | 43.6 ±0.8 |
| SA | 43.0 ±0.0 | 37.6 ±3.5 | 37.1 ±2.4 | 47.3 ±2.0 | 42.2 ±3.1 | 38.3 ±4.5 | 38.1 ±1.4 | 33.7 ±1.1 | 79.2 ±1.6 | 37.3 ±1.5 | 33.4 ±1.4 | 78.2 ±2.8 | 45.4 ±0.8 |
| FLDA-L | 41.9 ±0.9 | 42.7 ±2.1 | 41.1 ±2.0 | 52.3 ±1.2 | 48.9 ±2.4 | 42.9 ±1.7 | 33.6 ±1.8 | 31.8 ±1.8 | 75.8 ±3.1 | 36.3 ±2.0 | 32.6 ±0.7 | 75.7 ±2.1 | 46.3 ±0.7 |
| FLDA-Q | 42.8 ±1.5 | 42.0 ±1.8 | 40.6 ±2.0 | 52.6 ±1.4 | 47.6 ±1.5 | 43.4 ±1.8 | 32.5 ±1.6 | 29.5 ±4.0 | 59.9 ±15.4 | 36.9 ±1.2 | 33.9 ±1.2 | 72.3 ±2.2 | 44.5 ±1.4 |
| CORAL | 40.3 ±1.6 | 38.7 ±2.8 | 38.3 ±3.7 | 47.9 ±1.6 | 40.3 ±3.4 | 40.2 ±4.1 | 38.2 ±1.2 | 33.8 ±0.9 | 81.7 ±1.8 | 38.8 ±0.9 | 35.0 ±0.8 | 84.0 ±1.7 | 46.4 ±1.0 |
| Ad-REM SVM | 33.3 ±2.2 | 39.5 ±5.1 | 39.3 ±5.6 | 49.1 ±4.6 | 44.0 ±4.6 | 48.7 ±5.4 | 37.2 ±1.9 | 30.2 ±1.7 | 80.0 ±2.8 | 38.6 ±1.3 | 32.4 ±1.5 | 73.0 ±2.5 | 45.4 ±1.6 |
| Ad-REM LR | 33.3 ±2.6 | 38.8 ±3.8 | 36.9 ±3.4 | 49.4 ±4.3 | 44.3 ±4.7 | 49.4 ±4.4 | 38.3 ±1.8 | 30.4 ±1.8 | 81.5 ±2.7 | 38.4 ±2.0 | 32.3 ±2.2 | 75.7 ±2.2 | 45.7 ±1.2 |
| ResNet 50 | | | | | | | | | | | | | |
| Source SVM | 89.0 ±1.2 | 91.0 ±2.4 | 89.1 ±2.4 | 93.5 ±0.8 | 91.1 ±1.9 | 86.0 ±2.6 | 88.4 ±1.0 | 85.9 ±1.1 | 97.9 ±1.0 | 88.9 ±0.7 | 85.4 ±1.0 | 100.0 ±0.1 | 90.5 ±0.5 |
| Source LR | 89.8 ±1.0 | 92.2 ±1.8 | 90.1 ±1.8 | 93.9 ±0.7 | 90.6 ±1.9 | 86.3 ±2.4 | 88.8 ±1.2 | 86.2 ±1.0 | 98.0 ±0.9 | 89.3 ±0.7 | 85.0 ±0.8 | 99.9 ±0.2 | 90.9 ±0.5 |
| SA | 88.6 ±1.7 | 89.9 ±3.5 | 88.3 ±2.8 | 93.2 ±1.0 | 90.4 ±2.0 | 88.8 ±2.7 | 88.4 ±1.9 | 85.0 ±1.5 | 97.8 ±1.2 | 89.5 ±1.2 | 84.3 ±1.1 | 99.9 ±0.2 | 90.3 ±0.7 |
| FLDA-Q | 87.8 ±1.6 | 90.1 ±3.1 | 86.3 ±2.5 | 93.7 ±0.9 | 90.7 ±2.5 | 85.7 ±3.4 | 88.5 ±2.8 | 84.2 ±2.7 | 97.5 ±1.0 | 89.9 ±2.2 | 83.9 ±2.3 | 99.8 ±0.4 | 89.8 ±0.8 |
| CORAL | 88.8 ±1.4 | 93.2 ±2.9 | 90.5 ±2.1 | 94.2 ±0.7 | 92.5 ±2.8 | 90.8 ±2.7 | 92.9 ±1.0 | 87.4 ±1.2 | 98.1 ±1.1 | 92.1 ±0.8 | 85.9 ±0.9 | 100.0 ±0.0 | 92.2 ±0.6 |
| Ad-REM SVM | 93.2 ±0.4 | 98.8 ±2.2 | 98.6 ±1.2 | 95.2 ±0.6 | 98.7 ±2.2 | 98.1 ±1.3 | 95.9 ±0.2 | 94.2 ±0.3 | 98.7 ±1.2 | 95.9 ±0.2 | 93.6 ±0.2 | 100.0 ±0.0 | 96.7 ±0.3 |
| Ad-REM LR | 93.4 ±0.4 | 98.9 ±1.5 | 98.9 ±1.1 | 95.6 ±0.6 | 98.1 ±2.1 | 97.2 ±1.4 | 96.0 ±0.2 | 94.3 ±0.2 | 98.6 ±1.3 | 95.9 ±0.2 | 93.7 ±0.2 | 100.0 ±0.1 | 96.7 ±0.3 |

Table 4: Accuracy on the Office-Caltech 10 dataset, using the full source domain for training.

| | A→C | A→D | A→W | C→A | C→D | C→W | D→A | D→C | D→W | W→A | W→C | W→D | avg |
|---------------|-------------|-------------|-------------|-------------|-------------|-------------|-------------|-------------|-------------|-------------|-------------|--------------|-------------|
| SURF features | | | | | | | | | | | | | |
| Source SVM | 41.0 | 40.1 | 42.0 | 52.7 | 45.9 | 47.5 | 33.0 | 32.1 | 75.9 | 38.4 | 34.6 | 75.2 | 46.5 |
| Source LR | 42.3 | 40.1 | 39.7 | 54.6 | 45.2 | 49.5 | 35.9 | 32.2 | 82.7 | 37.9 | 34.0 | 79.6 | 47.8 |
| SA | 37.4 | 36.3 | 39.0 | 44.9 | 39.5 | 41.0 | 32.9 | 34.3 | 65.1 | 34.4 | 31.0 | 62.4 | 41.5 |
| FLDA-L | 41.5 | 45.9 | 42.0 | 49.5 | 48.4 | 44.1 | 31.7 | 34.1 | 75.6 | 35.3 | 33.8 | 72.6 | 46.2 |
| FLDA-Q | 43.5 | 43.3 | 40.7 | 53.5 | 44.6 | 45.1 | 30.8 | 31.2 | 73.2 | 35.2 | 32.1 | 75.8 | 45.7 |
| CORAL | 45.1 | 39.5 | 44.4 | 52.1 | 45.9 | 46.4 | 37.7 | 33.8 | 84.7 | 35.9 | 33.7 | 86.6 | 48.8 |
| Ad-REM SVM | 38.4 | 44.6 | 42.0 | 52.9 | 45.2 | 49.2 | 39.2 | 29.9 | 84.1 | 39.8 | 34.5 | 73.9 | 47.8 |
| Ad-REM LR | 41.1 | 43.3 | 43.4 | 57.1 | 45.2 | 53.6 | 41.5 | 30.8 | 86.8 | 37.9 | 30.3 | 78.3 | 49.1 |
| ResNet 50 | | | | | | | | | | | | | |
| Source SVM | 91.0 | 88.5 | 87.5 | 94.1 | 94.9 | 87.8 | 90.0 | 86.1 | 98.6 | 89.1 | 85.9 | 100.0 | 91.1 |
| Source LR | 91.7 | 91.7 | 92.5 | 93.8 | 93.6 | 85.8 | 88.7 | 85.8 | 98.0 | 89.7 | 85.6 | 100.0 | 91.4 |
| SA | 89.7 | 93.0 | 90.8 | 94.6 | 91.1 | 93.2 | 89.8 | 84.1 | 99.0 | 88.9 | 84.3 | 100.0 | 91.5 |
| FLDA-Q | 91.1 | 93.6 | 92.2 | 94.5 | 94.3 | 89.5 | 90.3 | 86.3 | 97.6 | 90.3 | 83.7 | 100.0 | 91.9 |
| CORAL | 85.9 | 91.1 | 89.8 | 94.3 | 93.0 | 93.2 | 92.8 | 86.8 | 98.6 | 90.9 | 85.5 | 100.0 | 91.8 |
| Ad-REM SVM | 92.9 | 97.5 | 98.0 | 95.5 | 99.4 | 98.3 | 95.9 | 94.7 | 99.7 | 95.8 | 93.6 | 100.0 | 96.8 |
| Ad-REM LR | 93.1 | 97.5 | 99.3 | 95.6 | 97.5 | 97.3 | 96.0 | 94.2 | 99.7 | 96.1 | 93.4 | 100.0 | 96.6 |

Table 5: Accuracy on the Office 31 dataset.

| | A→D | A→W | D→A | D→W | W→A | W→D | avg |
|--|-------------|-------------|-------------|-------------|-------------|--------------|-------------|
| DECAF-fc7 features | | | | | | | |
| Source SVM | 47.6 | 46.0 | 46.6 | 85.4 | 41.5 | 90.8 | 59.6 |
| Source LR | 53.0 | 50.2 | 44.1 | 85.1 | 42.0 | 89.4 | 60.6 |
| SA | 46.2 | 42.5 | 39.3 | 78.9 | 36.3 | 80.6 | 54.0 |
| FLDA-Q | 54.2 | 50.5 | 40.4 | 80.3 | 38.4 | 86.5 | 58.4 |
| CORAL | 57.1 | 53.1 | 51.1 | 94.6 | 47.3 | 98.2 | 66.9 |
| Ad-REM SVM | 51.6 | 53.1 | 46.8 | 86.3 | 54.7 | 92.8 | 64.2 |
| Ad-REM LR | 58.6 | 57.5 | 49.6 | 86.6 | 50.4 | 90.8 | 65.6 |
| ResNet 50 | | | | | | | |
| Source SVM | 76.9 | 73.8 | 60.3 | 97.5 | 59.4 | 100.0 | 78.0 |
| Source LR | 76.1 | 73.6 | 61.0 | 97.5 | 60.3 | 100.0 | 78.1 |
| SA | 76.7 | 75.5 | 62.2 | 97.9 | 60.3 | 100.0 | 78.8 |
| FLDA-Q | 76.3 | 75.5 | 59.9 | 97.5 | 58.6 | 99.8 | 77.9 |
| CORAL | 78.9 | 76.9 | 59.7 | 98.2 | 59.9 | 100.0 | 78.9 |
| Ad-REM SVM | 86.9 | 89.4 | 72.6 | 99.0 | 74.0 | 99.8 | 87.0 |
| Ad-REM LR | 88.0 | 87.0 | 72.8 | 99.0 | 72.9 | 100.0 | 86.6 |
| Deep Neural Networks (based on ResNet) | | | | | | | |
| DDC | 62.2 | 75.6 | 61.5 | 96.0 | 76.5 | 98.2 | 78.3 |
| DAN | 63.6 | 80.5 | 62.8 | 97.1 | 78.6 | 99.6 | 80.4 |
| RTN | 66.2 | 84.5 | 64.8 | 96.8 | 77.5 | 99.4 | 81.5 |
| RevGrad | 68.2 | 82.0 | 67.4 | 96.9 | 79.7 | 99.1 | 82.2 |
| JAN-A | 69.2 | 86.0 | 70.7 | 96.7 | 85.1 | 99.7 | 84.6 |

Table 6: Accuracy on the Cross Dataset Testbed.

| | C→I | C→S | I→C | I→S | S→C | S→I | avg |
|-------------------------------|-------------|-------------|-------------|-------------|-------------|-------------|-------------|
| DECAF-fc7 features | | | | | | | |
| Source SVM | 65.1 | 21.4 | 74.6 | 23.2 | 27.5 | 29.9 | 40.3 |
| Source LR | 64.1 | 21.3 | 74.6 | 23.7 | 24.6 | 27.6 | 39.3 |
| SA | 43.7 | 13.9 | 52.0 | 15.1 | 15.8 | 14.3 | 25.8 |
| FLDA-Q | 65.5 | 21.9 | 74.8 | 24.6 | 26.4 | 28.0 | 40.2 |
| CORAL | 66.2 | 22.9 | 74.7 | 25.4 | 26.9 | 25.2 | 40.2 |
| Ad-REM SVM | 65.8 | 20.4 | 75.9 | 25.1 | 35.1 | 39.1 | 43.6 |
| Ad-REM LR | 67.8 | 22.5 | 76.1 | 24.5 | 32.6 | 39.8 | 43.9 |
| DECAF-fc7 features, rectified | | | | | | | |
| Source SVM | 68.7 | 22.4 | 76.2 | 24.9 | 29.5 | 30.5 | 42.0 |
| Source LR | 70.5 | 23.8 | 78.1 | 25.5 | 31.1 | 34.1 | 43.8 |
| SA | 68.8 | 23.0 | 74.9 | 24.9 | 30.5 | 31.1 | 42.2 |
| FLDA-Q | 69.7 | 23.7 | 77.0 | 25.0 | 28.3 | 30.5 | 42.4 |
| CORAL | 69.0 | 23.6 | 75.9 | 25.7 | 34.8 | 34.2 | 43.9 |
| Ad-REM SVM | 76.0 | 24.0 | 80.3 | 26.7 | 39.3 | 44.8 | 48.5 |
| Ad-REM LR | 76.3 | 26.6 | 81.0 | 28.9 | 44.2 | 49.2 | 51.1 |

References

- Massih-Reza Amini and Patrick Gallinari. Semi-supervised learning with an explicit label-error model for misclassified data. In *Proceedings of the 18th IJCAI*, pages 555–560, 2003.
- Shai Ben-David, John Blitzer, Koby Crammer, Fernando Pereira, et al. Analysis of representations for domain adaptation. *Advances in neural information processing systems*, 19:137, 2007.
- Shai Ben-David, John Blitzer, Koby Crammer, Alex Kulesza, Fernando Pereira, and Jennifer Wortman Vaughan. A theory of learning from different domains. *Machine learning*, 79(1-2):151–175, 2010.
- John Blitzer, Ryan McDonald, and Fernando Pereira. Domain adaptation with structural correspondence learning. In *Proceedings of the 2006 conference on empirical methods in natural language processing*, pages 120–128. Association for Computational Linguistics, 2006.
- John Blitzer, Mark Dredze, Fernando Pereira, et al. Biographies, bollywood, boom-boxes and blenders: Domain adaptation for sentiment classification. In *ACL*, volume 7, pages 440–447, 2007.
- Konstantinos Bousmalis, George Trigeorgis, Nathan Silberman, Dilip Krishnan, and Dumitru Erhan. Domain separation networks. In *Advances in Neural Information Processing Systems*, pages 343–351, 2016.
- Lorenzo Bruzzone and Mattia Marconcini. Domain adaptation problems: A dasvm classification technique and a circular validation strategy. *Pattern Analysis and Machine Intelligence, IEEE Transactions on*, 32(5):770–787, 2010.
- François Chollet et al. Keras. <https://github.com/fchollet/keras>, 2015.
- Sumit Chopra, Suhrid Balakrishnan, and Raghuraman Gopalan. Dlid: Deep learning for domain adaptation by interpolating between domains. In *ICML workshop on challenges in representation learning*, volume 2, 2013.
- Rong-En Fan, Kai-Wei Chang, Cho-Jui Hsieh, Xiang-Rui Wang, and Chih-Jen Lin. Liblinear: A library for large linear classification. *J. Mach. Learn. Res.*, 9:1871–1874, June 2008. ISSN 1532-4435.
- Basura Fernando, Amaury Habrard, Marc Sebban, and Tinne Tuytelaars. Unsupervised visual domain adaptation using subspace alignment. In *Proceedings of the 2013 IEEE International Conference on Computer Vision, ICCV '13*, pages 2960–2967, Washington, DC, USA, 2013. IEEE Computer Society. ISBN 978-1-4799-2840-8.
- Vojtech Franc, Alexander Zien, and Bernhard Schölkopf. Support vector machines as probabilistic models. In *Proceedings of the 28th International Conference on Machine Learning (ICML-11)*, pages 665–672, 2011.
- Yaroslav Ganin and Victor Lempitsky. Unsupervised domain adaptation by backpropagation. In *International Conference on Machine Learning*, pages 1180–1189, 2015.
- Yaroslav Ganin, Evgeniya Ustinova, Hana Ajakan, Pascal Germain, Hugo Larochelle, François

- Laviolette, Mario Marchand, and Victor Lempitsky. Domain-adversarial training of neural networks. *Journal of Machine Learning Research*, 17(59):1–35, 2016.
- Pascal Germain, Amaury Habrard, François Laviolette, and Emilie Morvant. A new PAC-Bayesian perspective on domain adaptation. In *International Conference on Machine Learning (ICML)*, 2016.
- Zoubin Ghahramani and Michael I Jordan. Supervised learning from incomplete data via an em approach. In *Advances in neural information processing systems*, pages 120–127, 1994.
- Boqing Gong, Yuan Shi, Fei Sha, and Kristen Grauman. Geodesic flow kernel for unsupervised domain adaptation. In *Computer Vision and Pattern Recognition (CVPR), 2012 IEEE Conference on*, pages 2066–2073. IEEE, 2012.
- Boqing Gong, Kristen Grauman, and Fei Sha. Connecting the dots with landmarks: Discriminatively learning domain-invariant features for unsupervised domain adaptation. In *ICML (1)*, pages 222–230, 2013.
- Yves Grandvalet and Yoshua Bengio. Entropy regularization. *Semi-supervised learning*, pages 151–168, 2006.
- Yves Grandvalet, Johnny Mariéthoz, and Samy Bengio. A probabilistic interpretation of svms with an application to unbalanced classification. In *Advances in Neural Information Processing Systems*, pages 467–474, 2006.
- Amaury Habrard, Jean-Philippe Peyrache, and Marc Sebban. Boosting for unsupervised domain adaptation. In *Joint European Conference on Machine Learning and Knowledge Discovery in Databases*, pages 433–448. Springer, 2013.
- Kaiming He, Xiangyu Zhang, Shaoqing Ren, and Jian Sun. Deep residual learning for image recognition. In *Proceedings of the IEEE conference on computer vision and pattern recognition*, pages 770–778, 2016.
- Thorsten Joachims. Transductive support vector machines. *Chapelle et al.(2006)*, pages 105–118, 2006.
- Wouter M Kouw, Laurens JP van der Maaten, Jesse H Krijthe, and Marco Loog. Feature-level domain adaptation. *Journal of Machine Learning Research*, 17(171):1–32, 2016.
- Yuanqing Li, Cuntai Guan, Huiqi Li, and Zhengyang Chin. A self-training semi-supervised svm algorithm and its application in an eeg-based brain computer interface speller system. *Pattern Recognition Letters*, 29(9):1285–1294, 2008.
- Mingsheng Long, Yue Cao, Jianmin Wang, and Michael Jordan. Learning transferable features with deep adaptation networks. In *Proceedings of The 32nd International Conference on Machine Learning*, pages 97–105, 2015.
- Mingsheng Long, Jianmin Wang, and Michael I Jordan. Deep transfer learning with joint adaptation networks. *arXiv preprint arXiv:1605.06636*, 2016a.
- Mingsheng Long, Jianmin Wang, and Michael I Jordan. Unsupervised domain adaptation with residual transfer networks. *arXiv preprint arXiv:1602.04433*, 2016b.

- Anna Margolis. A literature review of domain adaptation with unlabeled data. *Tec. Report*, pages 1–42, 2011.
- Geoffrey J McLachlan. Iterative reclassification procedure for constructing an asymptotically optimal rule of allocation in discriminant analysis. *Journal of the American Statistical Association*, 70(350):365–369, 1975.
- Kamal Nigam, Andrew McCallum, and Tom Mitchell. Semi-supervised text classification using em. *Semi-Supervised Learning*, pages 33–56, 2006.
- Sinno Jialin Pan and Qiang Yang. A survey on transfer learning. *IEEE Transactions on knowledge and data engineering*, 22(10):1345–1359, 2010.
- Vishal M Patel, Raghuraman Gopalan, Ruonan Li, and Rama Chellappa. Visual domain adaptation: A survey of recent advances. *IEEE signal processing magazine*, 32(3):53–69, 2015.
- Kate Saenko, Brian Kulis, Mario Fritz, and Trevor Darrell. Adapting visual category models to new domains. In *European conference on computer vision*, pages 213–226. Springer, 2010.
- Matthias Seeger. Learning with labeled and unlabeled data. Technical report, 2000.
- Ozan Sener, Hyun Oh Song, Ashutosh Saxena, and Silvio Savarese. Learning transferrable representations for unsupervised domain adaptation. In *Advances in Neural Information Processing Systems*, pages 2110–2118, 2016.
- Hidetoshi Shimodaira. Improving predictive inference under covariate shift by weighting the log-likelihood function. *Journal of statistical planning and inference*, 90(2):227–244, 2000.
- Karen Simonyan and Andrew Zisserman. Very deep convolutional networks for large-scale image recognition. *CoRR*, abs/1409.1556, 2014.
- Alexander J Smola, SVN Vishwanathan, and Thomas Hofmann. Kernel methods for missing variables. In *AISTATS*, 2005.
- Baochen Sun and Kate Saenko. Deep coral: Correlation alignment for deep domain adaptation. In *Computer Vision–ECCV 2016 Workshops*, pages 443–450. Springer, 2016.
- Baochen Sun, Jiashi Feng, and Kate Saenko. Return of frustratingly easy domain adaptation. In *Thirtieth AAAI Conference on Artificial Intelligence*, 2016.
- Songbo Tan, Xueqi Cheng, Yuefen Wang, and Hongbo Xu. Adapting naive bayes to domain adaptation for sentiment analysis. *Advances in Information Retrieval*, pages 337–349, 2009.
- Tatiana Tommasi and Tinne Tuytelaars. A testbed for cross-dataset analysis. In *European Conference on Computer Vision*, pages 18–31. Springer, 2014.
- Eric Tzeng, Judy Hoffman, Ning Zhang, Kate Saenko, and Trevor Darrell. Deep domain confusion: Maximizing for domain invariance. *arXiv preprint arXiv:1412.3474*, 2014.
- Eric Tzeng, Judy Hoffman, Trevor Darrell, and Kate Saenko. Simultaneous deep transfer across domains and tasks. In *Proceedings of the IEEE International Conference on Computer Vision*, pages 4068–4076, 2015.

Xu Zhang, Felix Xinnan Yu, Shih-Fu Chang, and Shengjin Wang. Deep transfer network: Unsupervised domain adaptation. *arXiv preprint arXiv:1503.00591*, 2015.